Evaluation of Surface vs Bulk Contributions in Sum-Frequency Vibrational Spectroscopy Using Reflection and Transmission Geometries†

ARTICLE · MARCH 2000

DOI: 10.1021/jp9933929

5 AUTHORS, INCLUDING:

Seok-Cheol Hong
Korea University
52 PUBLICATIONS **887** CITATIONS
SEE PROFILE

yi-ren Shen
China Medical University (ROC)
249 PUBLICATIONS **10,461** CITATIONS
SEE PROFILE

Evaluation of Surface vs Bulk Contributions in Sum-Frequency Vibrational Spectroscopy Using Reflection and Transmission Geometries†

Xing Wei, Seok-Cheol Hong, A. I. Lvovsky, Hermann Held, and Y. R. Shen*

Department of Physics, University of California, and Materials Sciences Division, Lawrence Berkeley National Laboratory, Berkeley, California 94720

Received: September 21, 1999; In Final Form: January 4, 2000

An experiment was designed to measure sum-frequency generation (SFG) spectra in both reflection and transmission. The result from an octadecyltrichlorosilane monolayer on a substrate reveals that while the resonant spectra in the two geometries both originate from the surface monolayer, the bulk substrate has a significant contribution to the nonresonant background in the transmitted spectra. Study of a polyethylene film also shows that the bulk contribution to the SFG spectra is only significant for the transmission geometry, exhibiting a resonant mode not observable in the reflected spectra.

I. Introduction

In recent years, surface vibrational spectroscopy via infrared−visible sum-frequency generation (SFG) has been developed into a powerful tool to study the structures of surfaces and interfaces.[1] As a second-order nonlinear optical process, SFG is forbidden under the electric-dipole approximation in a medium with inversion symmetry but is necessarily allowed at a surface or interface where the inversion symmetry is broken. This unique feature makes SFG extremely sensitive to the surface or interfacial structure. Among many useful applications of SFG surface spectroscopy, studies of the interfacial structure of neat materials are of particular interest since few other techniques can yield the same information. Polymer surface structure is one such example. With Gabor Somorjai, we have initiated the study of polymer surfaces by SFG. We have been able to deduce from measurements surface composition, surface orientation of molecular groups, surface structure, and their response to the environment for a number of polymers.[2−7]

In interpreting the observed SFG spectra in reflection, one usually assumes that the spectra originate from the top surface monolayer. From a general physical argument, however, we can only conclude that the bulk electric-quadrupole contribution from a centrosymmetric medium is smaller than, or of the same order of magnitude as, the surface contribution to SFG in reflection.[1,8] Without any prior knowledge about the surface structure, it is not clear whether the bulk contribution can always be neglected. To be certain, we need to know the surface and bulk contributions separately. This, in general, cannot be done.[8−10] However, from SFG measurements in both reflection and transmission directions,[11] we can obtain a good estimate of the bulk nonlinearity that allows us to judge whether it is negligible or not.

Section II discusses the theoretical background and assumptions behind our measurements. Section III presents the experimental scheme for measurements and comparison of reflected and transmitted SFG spectra. The technique has been applied to two different samples. The first one is a silane monolayer adsorbed on fused quartz (section IV) from which the reflected and transmitted SFG spectra appear to be well correlated as they should be. The other one is a polyethylene film (section V). There, the reflected and transmitted SFG spectra are significantly different, indicating that the bulk contribution is important for the transmitted SFG. We can then deduce the value of the bulk nonlinearity and show that its contribution to the reflected SFG is indeed negligible. In fact, the measured bulk nonlinearity also gives us an estimate of how weak the reflected SFG would have to be for the bulk contribution to be nonnegligible.

II. Theory

In a typical surface SFG experiment, two input laser beams at frequencies ω_1 and ω_2 overlap at a surface or interface to induce a surface nonlinear polarization

$$\mathbf{P}_S^{(2)}(\sigma_s) = \epsilon_0 \chi_S^D : \mathbf{E}(\omega_1)\,\mathbf{E}(\omega_2) \tag{1}$$

and generate a coherent SFG output at ω_s in two well-defined directions (reflection and transmission, see Figure 1). Both directions are determined by the requirement that the parallel (x) components of the input and output wave vectors are matched:

$$k_{1x} + k_{2x} = k_{sx} \tag{2}$$

Scanning ω_2 over the frequency range of the surface molecular vibrational modes yields an SFG spectrum.

For a centrosymmetric bulk medium, although its nonlinear susceptibility χ_B^D vanishes under the electric-dipole approximation, it still has a bulk nonlinear polarization resulting from electric-quadrupole contributions[1,8,10]

$$\mathbf{P}_B^{(2)}(\omega_s) = \epsilon_0 \chi^{Q1} : \nabla \mathbf{E}(\omega_1)\,\mathbf{E}(\omega_2) + \epsilon_0 \chi^{Q2} : \mathbf{E}(\omega_1)\,\mathbf{E}(\omega_2) - \epsilon_0 \nabla \cdot [\chi^{Q} : \mathbf{E}(\omega_1)\,\mathbf{E}(\omega_2)] \tag{3}$$

This general form has also included the magnetic dipole contribution.[12] If $\mathbf{E}(\omega_1)$ and $\mathbf{E}(\omega_2)$ can be treated as plane waves with wave vectors k_1' and k_2', then eq 3 becomes

† Part of the special issue "Gabor Somorjai Festschrift".

* To whom all correspondence should be addressed.

10.1021/jp9933929 CCC: $19.00
Published on Web 03/08/2000

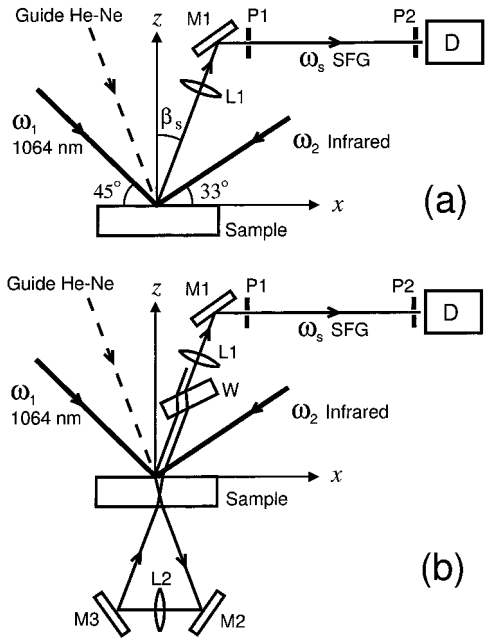

Figure 1. Experimental setup for measuring SFG in (a) reflection and (b) transmission. M1, M2, and M3, metal mirrors to reflect the SFG signal; P1 and P2, iris diaphragms to direct the SFG and the guide He−Ne beams; D, photodetector; L1, lens to image the beam spot on the sample surface to diaphragm P2; L2, lens to image the beam spot on the sample surface back to itself with a slight parallel shift; W, flat window to shift the SFG beam.

$$P_{\mathrm{B}i}^{(2)} = i\epsilon_0 \sum_{jlm} [\chi_{ijlm}^{\mathrm{Q1}} k'_{1m} + \chi_{ijlm}^{\mathrm{Q2}} k'_{2m} - \chi_{ijlm}^{\mathrm{Q}} (k'_{1m} + k'_{2m})] \cdot E_j(\omega_1)\, E_l(\omega_2) \quad (4)$$

This bulk contribution to SFG can be described in terms of an effective surface nonlinear susceptibility[13]

$$\chi_{ijk}^{\mathrm{SB}} = \sum_m \frac{\chi_{ijlm}^{\mathrm{Q}} (k'_{1m} + k'_{2m}) - \chi_{ijlm}^{\mathrm{Q1}} k'_{1m} - \chi_{ijlm}^{\mathrm{Q2}} k'_{2m}}{k'_{\mathrm{sz}} - k'_{1z} - k'_{2z}} \quad (5)$$

The absolute value of the denominator in eq 5 yields the factor $l_c = 1/|k'_{sz} - k'_{1z} - k'_{2z}|$, which is usually defined as the coherence length. Since k'_{sz} is positive and negative for the reflected and transmitted SFG, respectively, l_c is very different for the two geometries. By measuring SFG in both reflection and transmission directions, we can deduce some components of χ_{ijk}^{SB} and therefore obtain an estimate of χ^{Q}, χ^{Q1}, and χ^{Q2} if we assume their nonvanishing elements are of the same order of magnitude.

It is well-known that some part of the bulk contribution cannot be separated from the surface contribution in SFG and SHG (second-harmonic generation) measurements.[9] There are also extra bulk contributions arising from rapid variations of the fields and the structure at an interface.[10] They behave like a surface nonlinear susceptibility and also cannot be separated from $\chi_{\mathrm{S}}^{\mathrm{D}}$ experimentally. However, these are all electric-quadrupole in nature, and their contributions to the effective surface nonlinearity are of the same order as χ^{Q}. Thus deduction of an order-of-magnitude value of χ^{Q} from the measurement of χ_{ijk}^{SB} allows us to have an order-of-magnitude estimate of the importance of all the bulk contributions to SFG. In the following, we combine $\chi_{\mathrm{S}}^{\mathrm{D}}$ and the inseparable bulk contributions into one quantity $\chi_{\mathrm{S}}^{(2)}$ and express the total effective surface nonlinear susceptibility for SFG in the form

TABLE 1: Calculated SFG Exit Angle β_s for Different Infrared Beam Frequencies[a]

infrared wave number $\omega_2/(2\pi c)$, cm^{-1}	SFG exit angle β_s, deg
2800	20.6
2900	20.0
3000	19.5

[a] The "visible" beam ω_1 is at 1064 nm, and the incidence angles of ω_1 and ω_2 are 45° and 57° from the sample surface normal, respectively, as shown in Figure 1a.

$$\chi_{\mathrm{tot}}^{(2)} = \chi_{\mathrm{S}}^{(2)} + \frac{\chi_{\mathrm{B}}^{(2)}(k'_1, k'_2)}{k'_{\mathrm{sz}} - k'_{1z} - k'_{2z}} \quad (6)$$

III. Experiment

The experimental arrangement is depicted in Figure 1. The input beams, one at 1.064 μm, and the other tunable between 2.5 and 8 μm, were generated from a Nd:YAG laser and a laser-pumped optical parametric system. Both beams have a pulse width of ~15 ps, a repetition rate of 20 Hz, and a typical beam diameter of ~1 mm at the sample surface. Since alignment is crucial for this experiment, we give below a detailed account of our alignment procedure.

First, to align for the reflected SFG measurements (Figure 1a), we used a z-cut quartz reference sample to optimize the signal. The SFG reflection angle β_s varied with the input infrared wavelength (Table 1) but could be compensated by lens L1, which imaged the beam spot on the sample surface to pinhole P2 in front of the detector. A He−Ne laser beam was then directed to trace the SFG beam path into detector D with the help of pinholes P1 and P2. With the real sample replacing the reference sample, the alignment was done by adjusting the sample position such that the reflected 1.064 μm input beam and the He−Ne laser beam retraced their previous beam paths.

If the dispersion between the He−Ne and SFG wavelengths (633 and ~810 nm in our experiment, respectively) is negligible, the He−Ne laser beam used to trace the reflected SFG beam should also trace the transmitted SFG beam. Therefore, for alignment of the transmitted SFG measurements (Figure 1b), we used mirrors M2 and M3 underneath the sample to reflect the transmitted He−Ne guide beam into the same path defined by P1 and P2 for the reflected beam. To compensate for the variation of the SFG exit angle due to dispersion, we used another lens (L2) between M2 and M3 to image the beam spot on the sample surface 1:1 back onto itself. The transmitted and reflected He−Ne, and hence SFG, beams were then along the same path through P1 and P2 into the detector.

In the actual SFG measurements, we had to separate reflected and transmitted SFG signals. This was accomplished by a small parallel shift of M3 to the right that displaced the transmitted SFG beam slightly from the reflected SFG beam on their way to the detector. Then only the reflected SFG output could go through the pinholes to reach the detector. To measure the transmitted SFG, we inserted flat window W in front of L1 to compensate for the shift of the transmitted SFG beam caused by the shift of M3 and, at the same time, shift the reflected SFG beam away. Only the transmitted SFG output could then reach the detector.

The above alignment procedure was found to be reliable and easy to implement. Since the reflected and transmitted SFG signals were recorded by the same detection system, the results were amenable to quantitative comparison.

IV. Study of Octadecyltrichlorosilane Monolayer

We have measured SFG spectra in both reflection and transmission from an octadecyltrichlorosilane (OTS) monolayer on a fused quartz substrate. The sample was prepared by the usual self-assembly technique.[15] The thickness of the fused quartz substrate is about 3 mm, sufficient to eliminate the SFG contribution from the bottom surface. OTS has a long alkyl chain and is known to form a well-ordered self-assembled monolayer on glass. SFG spectra of the C−H stretch modes in reflection from such a monolayer were reported earlier.[16] In this case, because the resonant SFG signal originated from a surface monolayer, the reflected and transmitted spectra were expected to be correlated.

The surface nonlinear susceptibility $\chi_S^{(2)}$ of an OTS monolayer with $C_{\infty v}$ symmetry has only three independent nonvanishing elements:

$$\chi^{(2)}_{S,zzz}$$

$$\chi^{(2)}_{S,xxz} = \chi^{(2)}_{S,yyz}$$

$$\chi^{(2)}_{S,xzx} = \chi^{(2)}_{S,zxx} = \chi^{(2)}_{S,yzy} = \chi^{(2)}_{S,zyy}$$

In the last row, we have used the approximation $\chi^{(2)}_{S,ijk} = \chi^{(2)}_{S,jik}$ because ω_1 and ω_s are far away from electronic resonances.

Near vibrational resonances, $\chi_S^{(2)}$ takes the form

$$\chi_S^{(2)}(\omega_2) = \chi_S^{NR} + \sum_q \frac{\mathbf{A}_q}{\omega_2 - \omega_q + i\Gamma_q} \tag{7}$$

where χ_S^{NR} describes the nonresonant background and $\mathbf{A}_q$, ω_q, and Γ_q are the amplitude, resonant frequency, and damping constant, respectively, of the qth molecular vibrational mode.

In MKS units the SFG output intensity is given by[17]

$$I(\omega_s) = \frac{\omega_s^2}{8\epsilon_0 c^3 \cos^2\beta_s} |\chi^{(2)}_{tot,eff}|^2 I(\omega_1)\, I(\omega_2) \tag{8}$$

where $I(\omega_i)$ is the beam intensity at ω_i and $\chi^{(2)}_{tot,eff}$ is the total effective surface nonlinear susceptibility defined as

$$\chi^{(2)}_{tot,eff} = \chi^{(2)}_{S,eff} + \chi^{(2)}_{B,eff}$$

$$= [\mathbf{L}(\omega_s)\cdot\mathbf{e}_s]\cdot\chi^{(2)}_{tot}:\ [\mathbf{L}(\omega_1)\cdot\mathbf{e}_1][\mathbf{L}(\omega_2)\cdot\mathbf{e}_2] \tag{9}$$

with $\mathbf{e}_i$ being the unit polarization vector of the optical field at ω_i and $\mathbf{L}(\omega_i)$ being the tensorial Fresnel factor. In the present case, $\chi^{(2)}_{B,eff}$ comes from the fused quartz substrate.

The Fresnel factors at the center of our tuning range have been calculated and listed in Table 2. Because the tuning range is relatively small (200 cm^{-1}) in this experiment, the dispersion of Fresnel factors due to the variation of ω_2 can be neglected. Using these values, we can express all the surface effective nonlinear susceptibilities in terms of the three independent nonvanishing $\chi^{(2)}_{S,ijk}$ elements:

$$\chi^{(2)}_{S,eff}(ssp,R) = 0.47\chi^{(2)}_{S,xxz}$$

$$\chi^{(2)}_{S,eff}(ssp,T) = 0.56\chi^{(2)}_{S,xxz}$$

$$\chi^{(2)}_{S,eff}(ppp,R) = 0.25\chi^{(2)}_{S,zzz} - 0.42\chi^{(2)}_{S,xxz} + 0.19\chi^{(2)}_{S,xxx}$$

TABLE 2: Parameters of the Three Beams and the Calculated Fresnel Factors for the Air/Fused Quartz Interface[a]

	ω_s(R)	ω_s(T)	ω_1	ω_2
λ	810 nm	810 nm	1064 nm	3.4 μm
n	1.453	1.453	1.450	1.410
β	20.0°	20.0°	45°	57°
L_{xx}	0.83	0.97	0.92	1.02
L_{yy}	0.80	0.96	0.72	0.65
L_{zz}	1.17	0.97	1.08	0.98
$L_{xx}e_x$(p)	−0.78	0.91	0.65	−0.56
$L_{yy}e_y$(s)	0.80	0.96	0.72	0.65
$L_{zz}e_z$(p)	0.40	0.33	0.77	0.82

[a] (R) and (T) represent reflection and transmission, respectively. $\mathbf{L}(\omega_s, T)$ includes the transmission coefficient of the bottom surface of the fused quartz substrate. The dielectric constant of the surface monolayer $\epsilon' = 1$ was used for the calculation of L_{zz}.

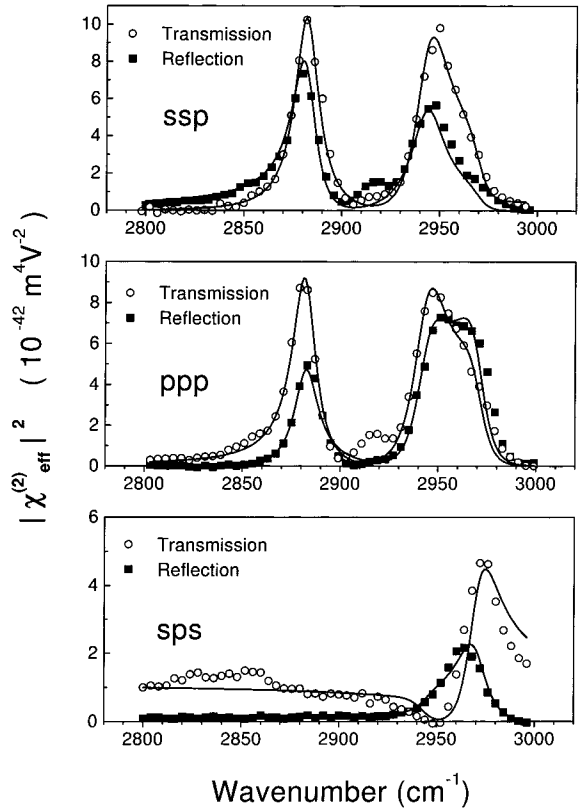

Figure 2. SFG spectra of an OTS monolayer on fused quartz. Points are experiment data, and the curves are theoretical fits.

$$\chi^{(2)}_{S,eff}(ppp,T) = 0.21\chi^{(2)}_{S,zzz} + 0.49\chi^{(2)}_{S,xxz} - 0.51\chi^{(2)}_{S,xzx}$$

$$\chi^{(2)}_{S,eff}(sps,R) = 0.40\chi^{(2)}_{S,szs}$$

$$\chi^{(2)}_{S,eff}(sps,T) = 0.48\chi^{(2)}_{S,xzx} \tag{10}$$

These equations show strict correlation between the reflected and transmitted SFG spectra from the surface contribution, in contrast to the effective bulk nonlinear susceptibility $\chi^{(2)}_{B,eff}$, which can be strongly enhanced by the longer coherence length in the transmission direction.

Figure 2 shows the reflected and transmitted SFG spectra obtained from the OTS monolayer. To take into account the different losses of signal in reflection and transmission, all spectra were normalized against the SFG intensity from a z-cut crystalline quartz reference sample (see Appendix A for details), which makes it possible to plot all spectra in MKS units. The reflected and transmitted spectra in Figure 2 seem to be

TABLE 3: Molecular Vibrational Modes on an OTS Monolayer and Their Corresponding Nonlinear Amplitudes Obtained from Fitting of the SFG Spectra

q	$\omega_q/(2\pi c)$, cm^{-1}	$\Gamma_q/(2\pi c)$, cm^{-1}	A_{xxz}[a]	A_{zzz}	A_{xzx}
s-CH_3	2882	7.5	7.9	1.2	0
Fermi-res.	2943	10.5	10.2	0.1	−1.5
a-CH_3	2970	9.5	−3.4	6.3	6.4

[a] The unit of A is 10^{-9} m^2 V^{-1} s^{-1}.

TABLE 4: Nonresonant Background Obtained from Fitting of the SFG Spectra of OTS in the Unit of 10^{-22} m^2 V^{-1}

	reflection	transmission
$\chi^{NR}_{tot,eff}$(ssp)	−3.4	2.8
$\chi^{NR}_{tot,eff}$(ppp)	−2.6	−0.7
$\chi^{NR}_{tot,eff}$(sps)	−3.2	10
$\chi^{NR}_{S,eff}$(sps)	−2.4	−3
$\chi^{NR}_{B,eff}$(sps)	−0.8	13

somewhat different, especially for the sps polarization combination (i.e., s-, p-, and s-polarized SFG output at ω_s, 1064 nm input at ω_1, and tunable infrared input at ω_2, respectively), but this can be explained by the different nonresonant bulk contributions $\chi^{(2)}_{B,eff}$ for the two different geometries. In fact, we were able to fit all the spectra (shown by the solid lines in Figure 2) using eqs 7 and 10 with the same set of $\mathbf{A}_q$, ω_q, and Γ_q values and different nonresonant contributions $\chi^{NR}_{tot,eff}$, as listed in Tables 3 and 4. The typical relative error of deduced $\mathbf{A}_q$ or $\chi^{(2)}$ in SFG is about 10%. The close fit in Figure 2 indicates that SFG spectra in reflection and transmission from the OTS monolayer are indeed very well correlated.

With the values of $\chi^{NR}_{tot,eff}$ in both reflection and transmission, we could further deduce $\chi^{NR}_{S,eff}$ and $\chi^{NR}_{B,eff}$. Here we take the sps polarization combination as an example. From eqs 6 and 9, we have

$$\chi^{(2)}_{S,eff}(sps) = L_{yy}(\omega_s)e_{sy}\chi^{(2)}_{S,yzy}L_{zz}(\omega_1)\,e_{1z}L_{yy}(\omega_2)e_{2y} \quad (11)$$

$$\chi^{(2)}_{B,eff}(sps) = \frac{L_{yy}(\omega_s)\,e_{sy}L_{yy}(\omega_2)e_{2y}}{k'_{sz}-k'_{1z}-k'_{2z}}[\chi^{(2)}_{B,yzy}L_{zz}(\omega_1)e_{1z}+\chi^{(2)}_{B,yxy}L_{xx}(\omega_1)e_{1x}] \quad (12)$$

Here, we have two nonvanishing components $\chi^{(2)}_{B,yzy}$ and $\chi^{(2)}_{B,yxy}$ contributing to the bulk term because, as shown by eq 5, $\chi^{(2)}_B$ depends linearly on the wave vectors k'_1 and k'_2, which break the inversion symmetry along the x- and z-axes. Equations 11 and 12 are valid for both resonant and nonresonant contributions. Only two parameters are different for the reflection and transmission geometries. One is $L_{yy}(\omega_s)e_{sy}$, which can be found in Table 2, and the other is $1/|k'_{sz}-k'_{1z}-k'_{2z}|$ which is equal to 49 and 720 nm for reflection and transmission, respectively. Inserting these values in eqs 11 and 12, we find

$$\chi^{(2)}_{tot,eff}(sps,R) = \chi^{(2)}_{S,eff}(sps,R)+\chi^{(2)}_{B,eff}(sps,R) = 0.52\{\chi^{(2)}_{S,yzy}L_{zz}(\omega_1)e_{1z}+49\ nm[\chi^{(2)}_{B,yzy}L_{zz}(\omega_1)e_{1z}+\chi^{(2)}_{B,yxy}L_{xx}(\omega_1)e_{1x}]\} \quad (13)$$

$$\chi^{(2)}_{tot,eff}(sps,T) = \chi^{(2)}_{S,eff}(sps,T)+\chi^{(2)}_{B,eff}(sps,T) = 0.62\{\chi^{(2)}_{S,yzy}L_{zz}(\omega_1)e_{1z}-720\ nm[\chi^{(2)}_{B,yzy}L_{zz}(\omega_1)e_{1z}+\chi^{(2)}_{B,yxy}L_{xx}(\omega_1)e_{1x}]\} \quad (14)$$

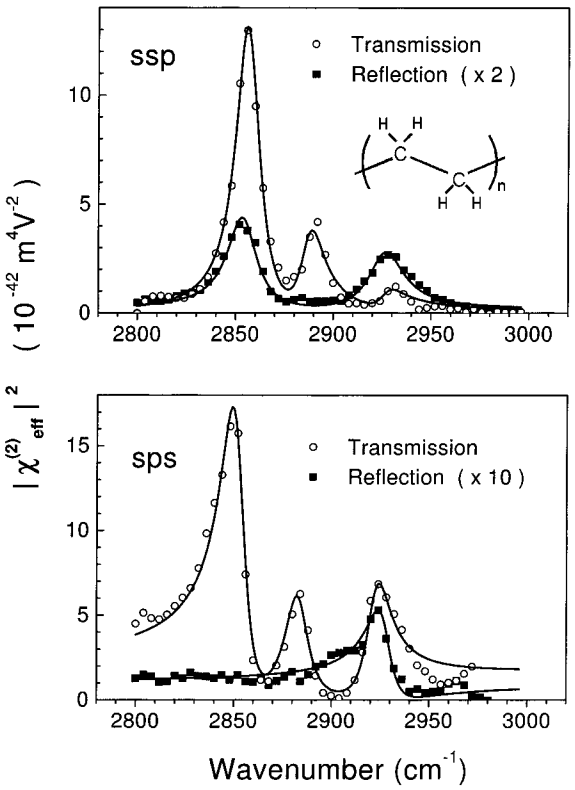

Figure 3. SFG spectra of a polyethylene film on fused quartz. The solid curves are theoretical fits.

which are again valid for both resonant and nonresonant contributions. Thus knowing the values of $\chi^{NR}_{tot,eff}$(sps,R) and $\chi^{NR}_{tot,eff}$(sps,T) listed in Table 4, we could solve eqs 13 and 14 and obtain the surface and bulk contributions $\chi^{NR}_{S,eff}$(sps) and $\chi^{NR}_{B,eff}$(sps) separately. Their values are also listed in Table 4.

V. Study of Polyethylene Film

We have also measured the reflected and transmitted SFG in the C−H stretch region from a thin film of polyethylene on a fused quartz plate. The molecular structure of polyethylene is shown in the inset of Figure 3. The reflected SFG spectra were reported in an earlier study, and they were found to be dominated by the surface contribution.[2] With transmitted SFG, we can determine the bulk contribution more quantitatively.

The polyethylene sample used in this experiment was prepared on fused silica substrate using the following technique. A grain of low-density polyethylene was sandwiched between fused silica and sodium chloride windows. It was heated until it completely melted. Then it was squeezed between the two windows to form a film of 100−200 μm thick. The "sandwich" was then cooled to room temperature and immersed in distilled water. Owing to dissolution, the NaCl window was separated from the film, and a smooth polyethylene surface appeared, suitable for optical measurements. The film thickness was sufficient to absorb most of the infrared energy to prevent the polymer/silica interface from contributing to SFG. Therefore the SFG signal we measured must come from the air/polymer interface and the neighboring polymer bulk within the infrared absorption length.

Figure 3 displays the SFG spectra of polyethylene for the ssp and sps polarization combinations. While the reflection SFG spectra are essentially the same as those published in ref 2, the transmission SFG spectra are very different and can be explained

only by the existence of the bulk contribution. The spectra show mainly three vibrational modes at 2850, 2884, and 2926 cm^{-1}. They can be assigned to the symmetric CH_2, Raman-active antisymmetric CH_2, and IR-active antisymmetric CH_2 stretch vibrations, respectively.[2,18,19] One remarkable feature is that the Raman-active antisymmetric CH_2 stretch mode appears in the transmitted SFG spectra but not in the reflected SFG spectra. Being Raman-active and infrared-forbidden, this vibrational mode can only be excited by the infrared field via electric-quadrupole excitation and therefore shows up only in the bulk contribution to SFG.

The significantly stronger SFG signal in the transmitted direction is due to a longer coherence length l_c that enhances the bulk contribution through the $\chi^{(2)}_B$ term in eq 6. From the measured spectra, we can obtain a rough estimate of $\chi^{(2)}_B$. Here we consider the CH_2 symmetric stretch mode in the sps polarization combination, which appears to be the strongest peak in the transmitted SFG spectrum. Since polyethylene has a refractive index ($\sim$1.5) very close to that of fused quartz, we can still use eqs 13 and 14 as a good approximation because the Fresnel factors and the coherence length in eqs 11 and 12 are not very sensitive to the refractive index. For example, varying n from 1.45 to 1.60 only changes $L_{yy}(\omega_s,\mathrm{R})$ in Table 2 from 0.80 to 0.75.

From Figure 3 we find that at the peak of the CH_2 symmetric stretch mode

$$|\chi^{(2)}_{\mathrm{tot,eff}}(\mathrm{sps,T})| \approx 4 \times 10^{-21}\ \mathrm{m^2\ V^{-1}}$$

$$|\chi^{(2)}_{\mathrm{tot,eff}}(\mathrm{sps,R})| \approx 0$$

By solving eqs 13 and 14, we obtain the effective bulk contribution in the reflection direction

$$|\chi^{(2)}_{\mathrm{B,eff}}(\mathrm{sps,R})| \approx 3 \times 10^{-22}\ \mathrm{m^2\ V^{-1}}$$

which is 1 order of magnitude smaller than the typical surface dipole contribution $|\chi^{(2)}_{\mathrm{S,eff}}(\mathrm{R})| \approx 10^{-21}\ \mathrm{m^2\ V^{-1}}$ on a vibrational resonance. This indicates that in the reflected SFG from polyethylene, the bulk contribution is indeed negligible.

The above value of $|\chi^{(2)}_{\mathrm{B,eff}}(\mathrm{R})|$ suggests that with the reflection geometry the bulk contribution is usually negligible as long as the SFG signal is reasonably strong (i.e., $|\chi^{(2)}_{\mathrm{tot,eff}}(\mathrm{R})| \gg 3 \times 10^{-22}\ \mathrm{m^2\ V^{-1}}$). This justifies the assumption in many cases that the reflected SFG spectra are dominated by surface contribution and can be used to probe surface structure.

VI. Conclusion

We have developed a scheme to measure both reflected and transmitted SFG spectra from the same sample and used them to estimate the relative contributions of surface and bulk to SFG. Measurements on an OTS monolayer adsorbed on fused quartz showed that the reflected and transmitted spectra originating from the monolayer are well correlated, while the nonresonant background resulting from the bulk contribution of the substrate is significant only in the transmitted spectra. That the bulk contribution is important only for transmitted SFG is also true in the case of polyethylene. A resonant mode that is only allowed in the bulk was found to appear only in the transmitted SFG spectra. Even though the bulk contribution is significant and easily detected in the transmitted SFG, our results suggest that the bulk contribution to the reflected SFG spectra is usually negligible.

TABLE 5: Parameters Used to Calculate $\chi^{(2)}_{\mathrm{eff}}$ of a z-Cut Quartz Crystal[a]

	ω_s(R)	ω_s(T)	ω_1	ω_2
λ	810 nm	810 nm	1064 nm	3.4 μm
$n = n_0$	1.539	1.539	1.534	1.49
β	20.0°	20.0°	45°	57°
L_{xx}	0.80	0.96	0.90	1.01
L_{yy}	0.77	0.95	0.68	0.61

[a] For convenience the birefringence (and also the optical activity) of the crystal is neglected and the refractive index of the ordinary wave n_0 is used for all polarizations.

Acknowledgment. This work was supported by the Director, Office of Energy Research, Office of Basic Energy Sciences, Materials Sciences Division of the U.S. Department of Energy under Contract No. DE-AC03-76SF00098, and a Max-Planck Society Research Award. H.H. gratefully acknowledges financial support from the Alexander-von-Humboldt Foundation.

Appendix A. Effective Surface Nonlinear Susceptibility of Crystalline Quartz

Equation 8 shows that we can measure $|\chi^{(2)}_{\mathrm{eff}}|^2$ of a sample by comparing its SFG intensity with that from a standard reference sample with a known $\chi^{(2)}_{\mathrm{eff}}$. In this experiment, we used a z-cut α-SiO_2 (quartz) crystal as our reference sample. The SFG signal from crystalline quartz is mainly from the bulk because it does not have inversion symmetry. Quartz crystal has D_3 symmetry with the following nonvanishing $\chi^{(2)}_{ijk}$ elements

$$\chi^{(2)}_{xxx} = -\chi^{(2)}_{xyy} = -\chi^{(2)}_{yyx} = -\chi^{(2)}_{yxy}$$

$$\chi^{(2)}_{xyz} = -\chi^{(2)}_{yxz}$$

$$\chi^{(2)}_{xzy} = -\chi^{(2)}_{yzx}$$

$$\chi^{(2)}_{zxy} = -\chi^{(2)}_{zyx}$$

among which $\chi^{(2)}_{xxx}$ (defined as $\chi^{(2)}_q$ below) and those equal to $\chi^{(2)}_{xxx}$ are much larger than the others.[20] In the following calculation we neglect the weaker ones. For the z-cut quartz crystal, the SFG intensity is maximized when the x-axis of the crystal is in the laser incidence plane. With this geometry, the absolute values of the effective surface nonlinear susceptibilities defined by eq 9 are

$$|\chi^{(2)}_{\mathrm{eff}}(\mathrm{ssp})| = g \cos\beta_2\, L_{yy}(\omega_s)\, L_{yy}(\omega_1)\, L_{xx}(\omega_2)\chi^{(2)}_q l_c$$

$$|\chi^{(2)}_{\mathrm{eff}}(\mathrm{sps})| = g \cos\beta_1\, L_{yy}(\omega_s)\, L_{xx}(\omega_1)\, L_{yy}(\omega_2)\chi^{(2)}_q l_c$$

$$|\chi^{(2)}_{\mathrm{eff}}(\mathrm{ppp})| = g \cos\beta_s \cos\beta_1 \cos\beta_2\, L_{xx}(\omega_s)\, L_{xx}(\omega_1)\, L_{xx}(\omega_2)\chi^{(2)}_q l_c \quad \text{(A1)}$$

Here, β and L_{ii} are the incidence angle and Fresnel factors, both listed in Table 5. $g = 2$ is a degeneracy constant that arises from the number of distinguishable permutations of the input frequencies.[20] l_c is the SFG coherence length, which, in our case, is approximately 46 and 755 nm for the reflection and transmission geometries, respectively.

Since in our experiment the SFG from crystalline quartz is nonresonant, we may neglect the dispersion and assume that

$$\chi_q^{(2)} = 2d_{11} \approx 8.0 \times 10^{-13}\frac{m}{V} \quad \text{(A2)}$$

where d_{11} refers to the nonlinear coefficient for second harmonic generation and its value for $\lambda = 1.064\ \mu$m found in ref 20 was used.

We then find from eqs A1

$$|\chi_{eff}^{(2)}(ssp,R)| = 2.1 \times 10^{-20}\frac{m^2}{V}$$

$$|\chi_{eff}^{(2)}(sps,R)| = 2.2 \times 10^{-20}\frac{m^2}{V}$$

$$|\chi_{eff}^{(2)}(ppp,R)| = 2.0 \times 10^{-20}\frac{m^2}{V}$$

$$|\chi_{eff}^{(2)}(ssp,T)| = 4.3 \times 10^{-19}\frac{m^2}{V}$$

$$|\chi_{eff}^{(2)}(sps,T)| = 4.5 \times 10^{-19}\frac{m^2}{V}$$

$$|\chi_{eff}^{(2)}(ppp,T)| = 3.8 \times 10^{-19}\frac{m^2}{V} \quad \text{(A3)}$$

References and Notes

(1) Shen, Y. R. In *Proceedings of the International School of Physics "Enrico Fermi", Course CXX, Frontiers in Laser Spectroscopy*; Hänsch, T. W., Inguscio, M., Eds.; North-Holland: Amsterdam, 1994; p 139.

(2) Zhang, D.; Shen, Y. R.; Somorjai, G. A. *Chem. Phys. Lett.* **1997**, *281*, 394.

(3) Zhang, D.; Ward, R. S.; Shen, Y. R.; Somorjai, G. A. *J. Phys. Chem.* **1997**, *B101*, 9060.

(4) Gracias, D. H.; Zhang, D.; Shen, Y. R.; Somorjai, G. A. *Tribol. Lett.* **1998**, *4*, 231.

(5) Zhang, D.; Gracias, D. H.; Ward, R.; Gauckler, M.; Tian, Y.; Shen, Y. R.; Somorjai, G. A. *J. Phys. Chem.* **1998**, *B102*, 6225.

(6) Gracias, D. H.; Zhang, D.; Lianos, L.; Ibach, W.; Shen, Y. R.; Somorjai, G. A. *J. Chem. Phys.* **1999**, *245*, 277.

(7) Wei, X.; Zhuang, X.; Hong, S.-C.; Goto, T.; Shen, Y. R. *Phys. Rev. Lett.* **1999**, *82*, 4256.

(8) Shen, Y. R. *Appl. Phys.* **1999**, *B68*, 295.

(9) Sipe, J. E.; Mizrahi, V.; Stegeman, G. I. *Phys. Rev.* **1987**, *B35*, 9091.

(10) Guyot-Sionnest, P.; Shen, Y. R. *Phys. Rev.* **1988**, *B38*, 7985.

(11) Superfine, R.; Huang, J. Y.; Shen, Y. R. *Phys. Rev. Lett.* **1991**, *66*, 1066.

(12) Pershan, P. S. *Phys. Rev.* **1963**, *130*, 919.

(13) See, for example: Shen, Y. R. *The Principles of Nonlinear Optics*; Wiley: New York, 1984; Chapter 25.

(14) Guyot-Sionnest, P.; Chen, W.; Shen, Y. R. *Phys. Rev.* **1986**, *B33*, 8254.

(15) Sagiv, J. *J. Am. Chem. Soc.* **1980**, *120*, 92.

(16) Guyot-Sionnest, P.; Superfine, R.; Hunt, J. H.; Shen, Y. R. *Chem. Phys. Lett.* **1988**, *144*, 1.

(17) If the intensities $I(\omega_s)$, $I(\omega_1)$, and $I(\omega_2)$ are defined in a medium with a dielectric function $\epsilon_1(\omega_i)$, eq 8 should be modified to (see, for example, ref 1).

$$I(\omega_s) = \frac{\omega_s^2|\chi_{tot,eff}^{(2)}|^2 I(\omega_1)\, I(\omega_2)}{8\epsilon_0 c^3 \cos^2\beta_s \sqrt{\epsilon_1(\omega_s)\,\epsilon_1(\omega_1)\,\epsilon_1(\omega_2)}}$$

Therefore, eq 8 is only valid with $\epsilon_1(\omega_i) = 1$, which is the case for vacuum or air. For the transmitted SFG signal, eq 8 is still valid if we define $I(\omega_s)$ as the intensity of the SFG beam in air after it propagates through the bottom surface of the fused quartz substrate. In this case the transmission coefficient at the bottom surface must be included properly to calculate the Fresnel factor $\mathbf{L}(\omega_s)$ for the transmission geometry.

(18) Hummel, D. O. *Polymer Spectroscopy*; Verlag Chemie: London, 1973.

(19) Bentley, P. A.; Hendra, P. J. *Spectrochim. Acta* **1995**, *A51*, 2125.

(20) Pressley, R. J., Ed. *Handbook of Lasers*; Chemical Rubber Co.: Cleveland, OH, 1971; pp 489, 497.